J|A|C|S
ARTICLES
Published on Web 05/25/2006

The Dewar Benzene Radical Cation and Its Ring-Opening Reaction

Thomas Bally,* Stephan Matzinger,§ and Pawel Bednarek

Contribution from the Department of Chemistry, University of Fribourg, Switzerland

Received January 10, 2006; E-mail: Thomas.Bally@unifr.ch

Abstract: The radical cation of Dewar benzene, **1**$^{\bullet+}$, has been generated and observed by optical spectroscopy in cryogenic matrices. **1**$^{\bullet+}$ distinguishes itself by a charge resonance band at 600 nm, very similar in shape and position to that observed for the related radical cation of norbornadiene. This coincidence indicates that in ground-state **1**$^{\bullet+}$ the odd electron is also located in a π-MO. The energy of the charge resonance transition, which is very sensitive to the dihedral angle between the four-membered rings in **1**$^{\bullet+}$, is predicted consistently too low by TD-DFT and CASPT2. Probably this angle is too large in the B3LYP and CASSCF geometries. As **1**$^{\bullet+}$ can be observed at 77 K, it must be separated by a barrier of at least 7−8 kcal/mol from its very exothermic decay to the radical cation of benzene, **2**$^{\bullet+}$. An analysis shows that the ring-opening of **1**$^{\bullet+}$ is a multistep proccess involving two avoided crossings between potential surfaces of different symmetry and electronic nature. Owing to the orbital symmetry-forbidden nature of the process, the energy of **1**$^{\bullet+}$ starts by increasing steeply on stretching the central C−C bond, but then the system undergoes a crossing to a $^2A_1$ surface which leads adiabatically to an excited state of **2**$^{\bullet+}$. Therefore, another avoided crossing must be transited before the molecule can decay on the ground-state surface of **2**$^{\bullet+}$. The rearrangement of **1**$^{\bullet+}$ to **2**$^{\bullet+}$ is an example of a "pseudodiabatic" thermal reaction that transits between potential surfaces representing very different electronic structures.

Introduction

Dewar benzene **1** has been the subject of many experimental and theoretical investigations. Despite the great exothermicity of its ring-opening to benzene **2** (84−85 kcal/mol according to calculations),[1] this process is relatively slow ($\Delta H^{\ddagger} = 23$ kcal/mol in solution[2]) because it cannot easily avoid the orbital symmetry-forbidden pathway that leads from **1** to **2** within the C_{2v} point group that is shared by the two compounds.[3] Thus, **1** is stable in solution at room temperature for hours and needs to be heated to 80 °C to achieve rapid decomposition. The hexamethyl derivative, **2-Me$_6$**, is even sufficiently stable ($\Delta H^{\ddagger} = 36.4$ kcal/mol[4]) to make it a commercial product.

Pericyclic reactions are usually greatly accelerated upon oxidation or reduction,[5] an effect that has been termed "electron-transfer catalysis".[6,7] Many examples of this effect have been documented and put to practical use in synthetic chemistry.[8] Especially, electrocyclic ring-opening reactions are prone to acceleration, to the extent that the radical cations of small ring compounds such as cyclobutene[9] and quadricyclane[10] may hardly be observed, even at low temperatures[9,11,12] and/or by time-resolved transient spectroscopy.[13,14]

In contrast to their neutral counterparts, where electronic ground states are invariably totally symmetric, the ground state wave functions of reactants and products in electrocyclic reactions of radical ions often transform differently with regard to the symmetry elements that are thought to be retained during the reaction.[15] This leads to avoided crossings along such symmetry-forbidden pathways or, if this possibility exists, to the choice of another, symmetry-allowed pathway for a radical ion rearrangement. A case in point is the cyclobutene radical cation where the ring-opening to the radical cation of *cis*-butadiene is symmetry forbidden both along the conrotatory and the disrotatory pathway.[9] As a consequence it decays by a completely different, symmetry-allowed pathway that leads directly to *trans*-butadiene radical cation.[16−18]

§ Present address: IBM Switzerland, Vulkanstrasse 106, CH-8010, Zürich.

(1) Norton, J. E.; Olson, L. P.; Houk, K. N. *J. Am. Chem. Soc.* **2006**, *128*, 7835.
(2) Breslow, R.; Napierski, J.; Schmidt, A. H. *J. Am. Chem. Soc.* **1972**, *94*, 5906.
(3) Goldstein, M. J.; Leight, R. S. *J. Am. Chem. Soc.* **1977**, *99*, 8112.
(4) Oth, J. F. M. *Recl. Trav. Chim. Pays-Bas* **1968**, *87*, 1185.
(5) Bauld, N. L.; Bellville, D. J.; Harirchian, B.; Lorenz, K. T.; Pabon, R. A.; Reynolds, D. W.; Wirth, D. D.; Chiou, H. S.; Marsh, B. K. *Acc. Chem. Res.* **1987**, *20*, 371.
(6) Chanon, M.; Tobe, M. L. *Angew. Chem., Int. Ed. Engl.* **1982**, *21*, 1.
(7) Bauld, N. L. *Adv. Electron-Transfer Chem.* **1992**, *2*, 1.
(8) Schmittel, M.; A., B. *Angew. Chem., Int. Ed. Engl.* **1997**, *36*, 2551.
(9) Aebischer, J.-N.; Bally, T.; Roth, K.; Haselbach, E.; Gerson, F.; Qin, X.-Z. *J. Am. Chem. Soc.* **1989**, *111*, 7909.
(10) Haselbach, E.; Bally, T.; Lanyiova, Z.; Baertschi, P. *Helv. Chim. Acta* **1979**, *62*, 583.
(11) Chen, G. F.; Wang, J. T.; Williams, F.; Belfield, K. D.; Baldwin, J. E. *J. Am. Chem. Soc.* **1991**, *113*, 9853.
(12) Cromack, K. R.; Werst, D. W.; Barnabas, M. V.; Trifunac, A. D. *Chem. Phys. Lett.* **1994**, *218*, 485.
(13) Gebicki, J. L.; Gebicki, J.; Mayer, J. *Radiat. Phys. Chem.* **1987**, *30*, 165.
(14) Ishiguro, K.; Khudyakov, I. V.; McGarry, P. F.; Turro, N. J.; Roth, H. D. *J. Am. Chem. Soc.* **1994**, *116*, 6933.
(15) Haselbach, E.; Bally, T.; Lanyiova, Z. *Helv. Chim. Acta* **1979**, *62*, 577.
(16) Wiest, O. *J. Am. Chem. Soc.* **1997**, *119*, 5713.
(17) Sastry, G. N.; Bally, T.; Hrouda, V.; Carsky, P. *J. Am. Chem. Soc.* **1998**, *120*, 9323.
(18) Swinarski, D. J.; Wiest, O. *J. Org. Chem.* **2000**, *65*, 6708.

10.1021/ja060176m CCC: $33.50

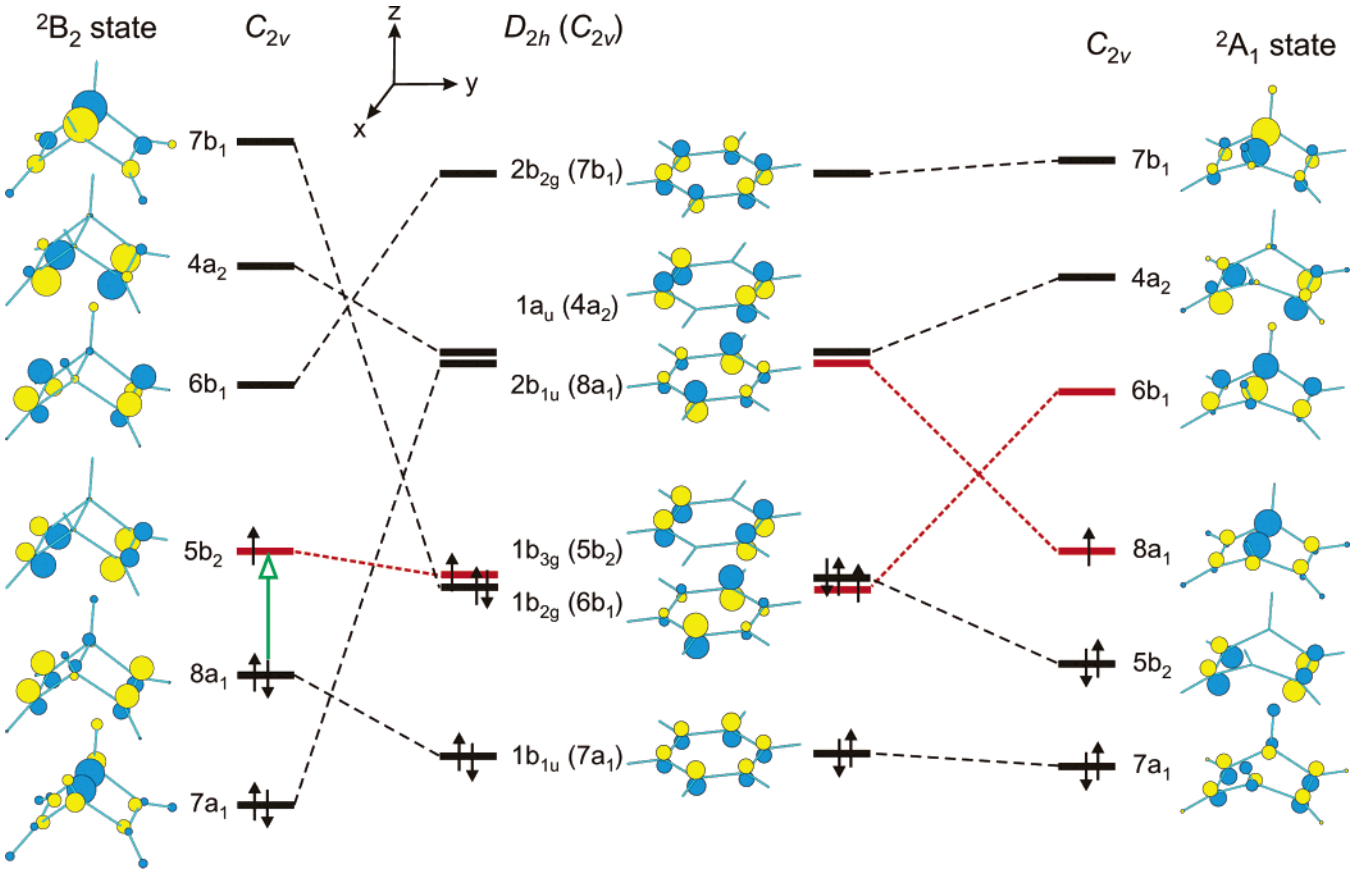

Figure 1. Orbital correlation diagram for the ring-opening of the radical cation of Dewar benzene (**1**$^{\bullet+}$) to that of benzene (**2**$^{\bullet+}$) from the $^2B_2$ state (left side) or the $^2A_1$ state of **1**$^{\bullet+}$ (right side). Note that the former reaction is state-symmetry allowed (the SOMOs correlate) in C_{2v} symmetry, whereas the latter is state-symmetry forbidden. The green arrow in the left diagram indicates the "charge resonance" absorption (Discussion, see text).

The cycloreversion of the radical cation of Dewar benzene **1**$^{\bullet+}$ to that of benzene **2**$^{\bullet+}$ is, however, a rather rare example of a radical cation electrocyclic reaction where the ground states of reactants and products are of the same symmetry, i.e., they correlate adiabatically along a C_{2v} symmetric ring-opening pathway. Nevertheless, the transformation is *orbital symmetry forbidden* along this pathway, similar to the neutral **1** → **2** rearrangement where the ground state of **1** correlates with a doubly excited state of **2** and vice versa.[19] Thus, the question arises whether **1**$^{\bullet+}$ has a way to avoid the high barrier that it faces along this orbital symmetry-forbidden pathway for its decay to **2**$^{\bullet+}$.[20]

A subtle but important point to be considered in the case of Dewar benzenes is, however, that their radical cations have two very close-lying ground states which are attained, respectively, by ejection of an electron from the antibonding combination of olefinic π-MOs ($^2B_2$)[21] or from a totally symmetric MO that represents a mixture of the bonding combination of olefinic π-MOs and a σ_{CC}-MO that is located in the central bridge ($^2A_1$).[20] The photoelectron spectrum of **1** shows that these two states are nearly degenerate at the geometry of neutral **1**, but Bieri et al. concluded from their analysis of this spectrum and from different calculations that the ground state of **1**$^{\bullet+}$ (at the geometry of neutral **1**) has B_2 symmetry.[20] If this is the case, then the ground state of **1**$^{\bullet+}$ and **2**$^{\bullet+}$ have the same symmetry (actually, **2**$^{\bullet+}$ has a degenerate ground state in D_{6h}, the components of which can be classified as $^2B_1$ and $^2B_2$ within the C_{2v} point group and which interconvert very rapidly on the very flat Jahn−Teller surface of **2**$^{\bullet+}$[22]). Conversely, in the $^2A_1$ state, the singly occupied MO (SOMO) of **1**$^{\bullet+}$ correlates with a virtual MO of **2**$^{\bullet+}$; hence, the ground state of **1**$^{\bullet+}$ correlates adiabatically with an *excited state* of **2**$^{\bullet+}$ (see right side of Figure 1).

In the radical cation of hexamethyl Dewar benzene, **1-Me$_6$**$^{\bullet+}$, we find the same states, this time separated more clearly in the photoelectron spectrum[20] except that in this case Bieri et al. posited that the ordering of states is inverted, i.e., $^2A_1$ below $^2B_2$, at the geometry of neutral **1-Me$_6$**.[20] After some claims to the effect that the $^2B_2$ and the $^2A_1$ states of **1-Me$_6$**$^{\bullet+}$ may coexist (or exist as separate entities),[23,24] several independent experiments have, however, converged on demonstrating that the ground state of **1-Me$_6$**$^{\bullet+}$ at its equilibrium geometry is $^2B_2$[21,25−27] In fact, it has been possible to observe **1-Me$_6$**$^{\bullet+}$ by optical[28]

(19) Halevi, E. A. *Angew. Chem., Int. Ed. Engl.* **1976**, *10*, 593.
(20) As the ionization energies of **1** and **2** are very similar (9.4 vs 9.25 eV, see: Bieri, G.; Heilbronner, E.; Kobayashi, T.; Schmelzer, A. J.; Goldstein, M.; Leight, R. S.; Lipton, M. S. *Helv. Chim. Acta* **1976**, *59*, 2657), the ring-opening of **1**$^{\bullet+}$ is similarly exothermic as that of **1**.
(21) In some publications, the HOMO of **1** (and hence the symmetry of the ground state of **1**$^{\bullet+}$) is desigated as b_1. Whether it is b_1 or b_2 depends on the choice of the *x* and *y* axis which is arbitrary in the C_{2v} point group. We adhere in this paper to the choice made by the authors of the accompanying paper.
(22) Koeppel, H.; Baldea, I.; Szalay, P. G. *Adv. Quantum Chem.* **2003**, *44*, 199.
(23) Roth, H. D.; Schilling, M. L. M.; Raghavachari, K. *J. Am. Chem. Soc.* **1984**, *106*, 4446.
(24) Rhodes, C. J. *J. Am. Chem. Soc.* **1988**, *110*, 8567.
(25) Arnold, A.; Gerson, F. *J. Am. Chem. Soc.* **1990**, *112*, 2027.
(26) Qin, Q.-Z.; Trifunac, A. D. *J. Phys. Chem.* **1990**, *94*, 4751.
(27) Williams, F.; Guo, Q. X.; Nelsen, S. F. *J. Am. Chem. Soc.* **1990**, *112*, 2028.
(28) Marcinek, A. *J. Phys. Chem. A* **1998**, *102*, 7761.

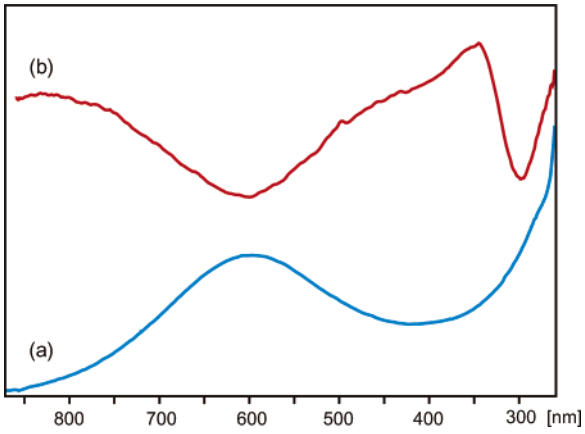

Figure 2. Optical difference spectra for the ionization of **1** in a Freon glass at 77 K (blue trace a), and for the subsequent bleaching of the resulting radical cation by 488−515 nm irradiation (red trace b). The corresponding spectra obtained in Ar matrices are given in Figure S1 of the Supporting Information.

and ESR spectroscopy in low-temperature matrices,[29] and by different forms of transient spectroscopy on the nanosecond time scale.[23,30,31] We therefore decided to investigate and see if it would be possible to characterize the parent compound, $\mathbf{1}^{\bullet+}$, by subjecting **1** to ionization in solid matrices.

It is the purpose of this paper to show that this is actually the case, and to explain in qualitative terms why $\mathbf{1}^{\bullet+}$ resists the very exothermic decay to $\mathbf{2}^{\bullet+}$at 77 K. Solid numbers that back these arguments are furnished in the accompanying computational study[1] which has been carried out independently of our work, and in the perspective of the application of **1-Me$_6$** as a system for imaging by quantum amplified isomerization. We also present for the first time the optical spectrum of $\mathbf{1}^{\bullet+}$ which shows that the ground state of this species must have, as in the case of $\mathbf{1\text{-}Me_6}^{\bullet+}$ and in the closely related case of the norbornadiene radical cation, B_2 symmetry.

Results and Discussion

UV/Vis Spectra and Assignment. Figure 2 shows the spectrum that was observed after ionization of **1** embedded in a Freon glass at 77 K (see Methods for details). A similar but much weaker spectrum was observed when **1** was subjected to ionization by X irradiation in Ar matrices (where the incipient radical cations are imparted with much more excess energy than in a Freon glass and, hence, have a smaller chance of survival; for the spectrum, see Supporting Information). Irradiation of the sample through a 500-nm cutoff filter with a 1000-W Ar plasma or a Hg/Xe lamp had no effect, but with a 4-W Ar ion laser in multimode (515−488 nm), the 600-nm band and an apparently associated sharper peak in the UV were bleached and replaced by a broad absorption such as is obtained on ionization of benzene in the same medium (difference spectrum B in Figure 2 and Figure S1 in the Supporting Information).

In Figure 3, the above-mentioned spectrum is compared, on an energy scale, with those of the closely related radical cations of norbornadiene, $\mathbf{3}^{\bullet+}$,[32] and that of hexamethyl Dewar benzene, $\mathbf{1\text{-}Me_6}^{\bullet+}$, which has previously been observed by Marcinek in

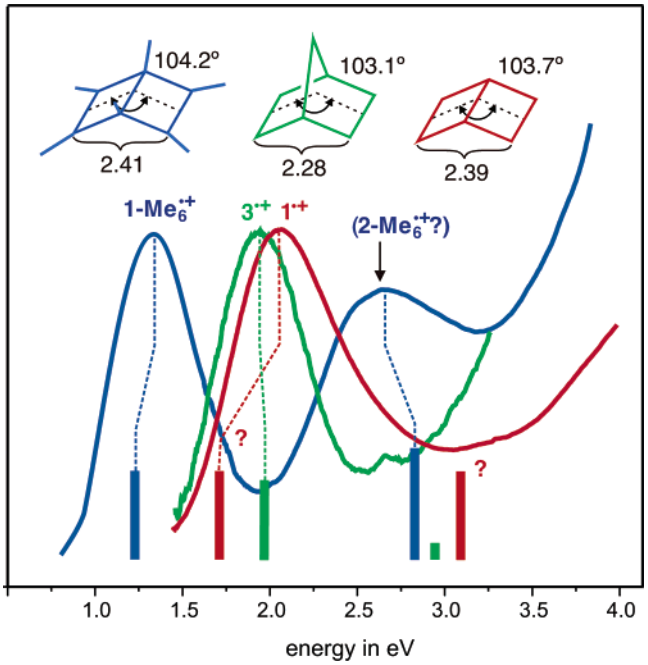

Figure 3. Optical spectra of $\mathbf{1}^{\bullet+}$, $\mathbf{1\text{-}Me_6}^{\bullet+}$,[28] and $\mathbf{3}^{\bullet+}$[32] in Freon glasses at 77 K, and predictions from excited-state CASSCF/CASPT2 calculations (cf. Table 1).

a slightly different organic medium.[28] The similarity in the shape of the first bands in the three spectra is striking, which suggests that the electronic transition responsible for these absorptions is of similar nature in all three cases. If the ground states of all three radical cations are the same, i.e., the SOMO corresponds to the antibonding combination of the olefinic π-MOs (the b_2 MO on the left side of Figure 1), then the transition corresponds to promotion of an electron from the bonding (a_1) to the antibonding combination of olefinic π-MOs (green arrow in Figure 1), which gives rise to what Badger and Brocklehurst once termed a "charge resonance band".[33] The energy at which this transition occurs depends primarily on the overlap between these two MOs, which in turn depends on the distance of the two bonds on which they are centered, and the angle ω under which they interact (cf. Figure 3).

Calculations show that these two parameters are very similar for $\mathbf{1}^{\bullet+}$ and $\mathbf{3}^{\bullet+}$ (in Figure 3, the numbers from B3LYP/6-31G* calculations are given), which would seem to explain the similarity of the two spectra. In $\mathbf{1\text{-}Me_6}^{\bullet+}$, the band maximum is, however, shifted by 0.74 eV to lower energy, although R and ω are very similar as in the parent compound $\mathbf{1}^{\bullet+}$.[1] This indicates that other factors (such as the degree of interaction with other, higher-lying electronic configurations of the same symmetry) contribute also to the position of the charge resonance band in such bis-olefinic radical cations. A clue to this can be found in Figure 1 which shows that $\mathbf{1}^{\bullet+}$ (and $\mathbf{1\text{-}Me_6}^{\bullet+}$) have *two* excited states of A_1 symmetry, the second one arising by promotion of an electron from the a_1 σ_{C-C} MO (lowest MO on the left side of Figure 1) to the SOMO. In contrast, the next A_1 state in $\mathbf{3}^{\bullet+}$ lies so high that it cannot contribute to the visible part of the spectrum.

In an attempt to shed some light on this electronic structure issue we carried out calculations on excited states of $\mathbf{1}^{\bullet+}$ by the CASSCF/CASPT2 method, based on geometries optimized at

(29) Rhodes, C. J. *J. Am. Chem. Soc.* **1984**, *106*, 253.
(30) Gebicki, J.; Marcinek, A.; Mayer, J. *J. Am. Chem. Soc.* **1989**, *111*, 3098.
(31) Qin, Q.-Z.; Werst, D. W.; Trifunac, A. D. *J. Am. Chem. Soc.* **1990**, *112*, 2026.
(32) Bally, T. *Chimia* **1994**, *48*, 378.
(33) Badger, B.; Brocklehurst, B. *Trans. Faraday Soc.* **1969**, 2576.

Table 1. Vertical Excitation Energies of $\mathbf{1}^{\bullet+}$ Calculated by the CASPT2 Method

state[a]	ΔE_{CASSCF}[b] eV	ΔE_{CASPT2} eV	reference weight[c]	λ nm	f[d]	major configurations CAS[e]
1^2B_1	0.00	0.00	0.78	–	–	91% ground config.
1^2A_1	1.81	1.71	0.77	725	8.8×10^{-2}	90% $8a_1 \rightarrow 5b_2$
2^2A_1	3.62	3.09	0.75	401	1.7×10^{-1}	90% $7a_1 \rightarrow 5b_2$
1^2B_2	3.45	3.32	0.75	373	0.0	77% $5b_2 \rightarrow 6b_1$

[a] Choice of axes see Figure 1. [b] (5,6) active space, state averaging over the lowest three roots in each symmetry. [c] Weight of the zero-order CASSCF in the CASPT2 wave function [d] Oscillator strength for electronic transition. [e] In terms of excitations in the space of orbitals depicted on the left-hand side of Figure 1.

Table 2. Vertical Excitation Energies of $\mathbf{1\text{-}Me_6}^{\bullet+}$ Calculated by the CASPT2 Method[a]

state[a]	ΔE_{CASSCF}[b] eV	ΔE_{CASPT2} eV	reference weight[c]	λ nm	f[d]	major configurations CAS[e]
$1\ ^2B_1$	0.00	0.00	0.64	–	–	95% ground config.
$1\ ^2A_1$	1.44	1.35	0.63	916	7.4×10^{-2}	91% $8a_1 \rightarrow 5b_2$
$2\ ^2A_1$	3.33	2.75	0.61	450	1.8×10^{-1}	91% $7a_1 \rightarrow 5b_2$
$1\ ^2B_2$	3.75	3.46	0.63	355	0.0	77% $5b_2 \rightarrow 6b_1$

[a] Choice of axes see Figure 1. [b] (5,6) active space, state averaging over the lowest three roots in each symmetry. [c] Weight of the zero-order CASSCF in the CASPT2 wave function [d] Oscillator strength for electronic transition. [e] In terms of excitations in the space of orbitals depicted on the left-hand side of Figure 1.

the B3LYP/6-31G* level, a combination of tools which has proven quite reliable in predicting UV/vis spectra of radical cations in many previous cases.[34] Tables 1 and 2 and the bars in Figure 3 sum up the results obtained by this method on the three compounds. Obviously the predictions are in excellent accord with the experimental spectra for $\mathbf{1\text{-}Me_6}^{\bullet+}$ and $\mathbf{3}^{\bullet+}$. They indicate that the broad band of $\mathbf{1\text{-}Me_6}^{\bullet+}$ at 470 nm (2.65 e4 eV) that Marcinek had attributed to $\mathbf{2\text{-}Me_6}^{\bullet+}$ (which indeed also absorbs there) is probably also due to $\mathbf{1\text{-}Me_6}^{\bullet+}$ and corresponds to excitation into the second $^2A_1$ state.

In contrast, the CASSCF/CASPT2 predictions for parent $\mathbf{1}^{\bullet+}$ are rather off the mark: the first band is predicted 0.36 eV too low in energy and the second one at an energy where the spectrum has a minimum (Table 1). As we can see no alternative but to assign the band peaking at 600 nm/2.2 eV to $\mathbf{1}^{\bullet+}$, we searched for reasons why this method could possibly fail in this particular case.

One of the reasons could be that the $^2B_2$ ground state of $\mathbf{1}^{\bullet+}$ (in contrast to those of $\mathbf{1\text{-}Me_6}^{\bullet+}$ and $\mathbf{3}^{\bullet+}$) suffers from severe symmetry breaking at the CASSCF level; in fact the geometry optimized by this method corresponds to a structure where the SOMO (and, hence, spin and charge) is localized in one of the two double bonds which consequently assumes a length of 1.406 Å (while that of the other one is 1.348 Å, close to the value in neutral **1**). That structure is 7.9 kcal/mol more stable than one where C_{2v} symmetry (and, hence, full delocalization of spin and charge over both double bonds) is enforced.

It appears that the symmetry breaking found at the CASSCF level is artifactual,[35] i.e. due to the neglect of dynamic electron correlation.[36] As the CASSCF wave function is the zero-order wave function on which the multiconfigurational MP2 treatment builds, it may be that perturbation theory fails to rectify the symmetry breaking and thus yields nonsensical results. Interestingly, increasing the active space in the CASSCF calculation to (13,12), and thus including a degree of dynamic electron correlation in the CASSCF wave function, moves the two transitions to higher energies, although still not into satisfactory agreement with experiment.

Another reason for the failure of theory in the case of $\mathbf{1}^{\bullet+}$ may be that the geometry, in particular the dihedral angle ω may not be predicted correctly by the B3LYP method. In fact, single-point CASPT2 or CCSD(T)/cc-pVTZ calculations on a series of geometries optimized for fixed values of ω ranging from 96° to 108° resulted in a curve whose minimum is close to 102°, i.e. almost 2° less than by B3LYP (see Figure S2 in the Supporting Information). As ω decreases, the predicted band positions move into better agreement with experment until at $\omega = 98°$ (a distortion that requires only 0.5 kcal/mol at the CCSD(T) level) the first band is predicted at 2.13 eV and the second at 3.57 eV, now in good accord with experiment (see Figure S3 in the Supporting Information).[37] Interestingly, the CASPT2 prediction for the gap between the $^2B_2$ and the two lowest $^2A_1$ states of $\mathbf{1}^{\bullet+}$at the geometry of *neutral* **1** is in perfect agreement with the photoelectron spectrum of **1**[20] (cf. Figure S4 in the Supporting Information). Perhaps the failure of CASSCF/CASPT2 to predict the spectrum of $\mathbf{1}^{\bullet+}$ with the usual accuracy is due to a combination of adverse circumstances in this particular case.

Potential Surfaces Involved in the Ring-Opening of $\mathbf{1}^{\bullet+}$. In the accompanying paper by Norton, Olson, and Houk (NOH),[1] the ground-state potential surface for the ring-opening of $\mathbf{1}^{\bullet+}$ to $\mathbf{2}^{\bullet+}$ has been carefully mapped. These authors have also shown that this conversion involves bypassing two conical intersections which they located at the CASSCF level. Our own calculations, which were conducted independently with methods similar to those used by NOH, are in full agreement with the

(34) (a) Bally, T.; Truttmann, L.; Dai, S.; Williams, F. *J. Am. Chem. Soc.* **1995**, *117*, 7916. (b) Truttmann, L.; Asmis, K. R.; Bally, T. *J. Phys. Chem.* **1995**. *99*, 17844. (c) Huben, K.; Zhu, Z.; Bally, T.; Gebicki, J. *J. Am. Chem. Soc.* **1997**, *119*, 2825. (d) Zhu, Z.; Bally, T.; Wirz, J.; Fülscher, M. *J. Chem. Soc., Perkin Trans. 2* **1998**, 1083. (e) Bally, T.; Carra, C.; Fülscher, M.; Zhu, Z. *J. Chem. Soc., Perkin Trans. 2* **1998**, 1759. (f) Marcinek, A.; Adamus, J.; Huben, K.; Gebicki, J.; Bartczak, T. J.; Bednarek, P.; Bally, T. *J. Am. Chem. Soc.* **2000**, 122, 437. (g) Bally, T.; Zhu, Z.; Wirz, J.; Fülscher, M.; Hasegawa, J.-Y. *J. Chem. Soc., Perkin Trans. 2* **2000**, 2311. (h) Bednarek, P.; Zhu, Z.; Bally, T.; Filipiak, T.; Marcinek, A.; Gebcki, J. *J. Am. Chem. Soc.* **2001**, *123*, 2377. (i) Müller, B.; Bally, T.; Gerson, F.; de Meijere, A.; von Seebach, M. *J. Am. Chem. Soc.* **2003**, *125*, 13776.

(35) Symmetry breaking occurs also at the ROHF or UHF levels, albeit to a much smaller extent (C_s structures are stabilized by 1.07 or 0.37 kcal/mol, respectively, relative to C_{2v} structures), whereas at the UMP2 and UQCISD levels geometry optimizations converge to structures of C_{2v} symmetry.

(36) Bally, T.; Borden, W. T. *Rev. Comput. Chem.* **1999**, *13*, 1.

(37) A reviewer has pointed out that the spectra of $\mathbf{1Me_6}^{\bullet+}$ and $\mathbf{3}^{\bullet+}$ are liable to be equally sensitive to ω as that of $\mathbf{1}^{i+}$. This is certainly the case, but it appears that in these compounds ω from B3LYP/6-31G* calculations happens to be correct (as gauged by the agreement of the predicted spectra with experiment). In $\mathbf{3}^{\bullet+}$ the potential is very steep along ω, so there is less room for an error in this parameter. Unfortunately, we were not able check by higher-level calculations whether ω is correct in $\mathbf{1Me_6}^{\bullet+}$ (which has a much flatter potential surface, as does $\mathbf{1}^{\bullet+}$).

Table 3. Energies of Stationary Points[a] on the Potential Surface for Ring-Opening $\mathbf{1}^{\bullet+} \rightarrow \mathbf{2}^{\bullet+}$

geometry →	B3LYP[b]		CASSCF[b]	
rel. energy →	B3LYP[b]	CCSD(T)[c]	CASSCF[b]	CCSD(T)[c]
$\mathbf{1}^{\bullet+}$ ($^2B_2$)	(0)	(0)	(0)	(0)
$^2B_2$-TS	*d*	–	31.05	44.09
$\mathbf{2}^{\bullet+}$ ($^2B_2$) (TS)	−73.91	−70.01	−92.04	−70.16
$\mathbf{2}^{\bullet+}$ ($^2B_1$) (min.)	−74.01	−69.88	−92.04	−70.05
$\mathbf{1}^{\bullet+}$ ($^2A_1$)	2.85	2.11	−7.57	2.92
$^2A_1$-TS	*d*	–	−0.61	18.67
$\mathbf{2}^{\bullet+}$ ($^2A_1$)	−1.42		−26.07	0.26
π/σ-TS ($^2B_2$−$^2A_1$)	7.99	7.60	1.08	6.42
CTS ($^2A_1$−$^2B_1$)	4.42	4.97	−7.54	6.78

[a] See Figure 4; absolute energies and Cartesian coordinates are given in the Supporting Information. [b] With the 6-31G* basis set. [c] With the cc-pVTZ basis set. [d] These transitions states are poorly described by single determinants; hence, they were not located by DFT.

picture elaborated by these authors and presented in the accompanying paper; hence, we relegate the details of our results to the Supporting Information. Instead, we use symmetry to show how the different potential surfaces connecting $\mathbf{1}^{\bullet+}$ and $\mathbf{2}^{\bullet+}$ evolve along the reaction coordinate (i.e. the distance of the central carbon atoms, r_{C-C}) and what exactly happens when the system transits between these surfaces (Table 3 and Figure 4).

From the orbital correlation diagram shown in Figure 1 it becomes evident that, analagous to the case of the rearrangement of **1** to **2**, the $^2B_2$ ground state of $\mathbf{1}^{\bullet+}$ correlates with a *doubly excited* state of $\mathbf{2}^{\bullet+}$ and vice versa (because the doubly occupied a1 σ_{C-C} MO of $\mathbf{1}^{\bullet+}$ correlates with the b_{1u} component of the unoccupied LUMO of $\mathbf{2}^{\bullet+}$). Hence, the reaction is orbital symmetry forbidden (as is the $\mathbf{1} \rightarrow \mathbf{2}$ rearrangement), which should lead to a substantial barrier on the $^2B_2$ surface that connects the ground states of $\mathbf{1}^{\bullet+}$ and $\mathbf{2}^{\bullet+}$ within C_{2v} symmetry. This is indeed what we found (see $^2B_2$-TS in Figure 4), but it turns out that this transition state is not of relevance to the chemistry of $\mathbf{1}^{\bullet+}$ because the $^2A_1$ state (which, according to the optical spectrum of $\mathbf{1}^{\bullet+}$ in Figure 2, lies about 2.2 eV above the $^2B_2$ state at its equilibrium geometry) falls below the $^2B_2$ state *before* $^2B_2$-TS is reached, so the system crosses over to the $^2A_1$ surface.

To avoid the $^2B_2/^2A_1$ conical intersection (appropriately called "CI σ/π" in the paper by NOH), and to effect this crossing, $\mathbf{1}^{\bullet+}$ must lose the plane of symmetry σ_A (marked blue in Figure 4), but may keep the perpendicular "red" symmetry plane σ_B (because the a_1 and b_2 SOMOs are both symmetric with regard to that plane). Indeed, the transition state ("σ/π-TS" in NOH's nomenclature) has C_s symmetry, but the lengths of the two double bonds differ by 6.7 pm (DFT) or 5.6 pm (CASSCF), respectively, and the carbon atoms on the longer of these two bonds are slightly pyramidalized. These distortions, which are in large part responsible for the remaining barrier, are brought about by the requirement that the coefficients on one of the double bonds in the π-SOMO must vanish, so that they can reemerge with the opposite sign on the $^2A_1$ surface (where the two components of the π-MO are in phase).

Physically this implies that, near the transition state, charge and spin must localize in one of the double bonds which therefore becomes much longer (ca. 1.39 Å by B3LYP) than the opposite one whose length corresponds to that of a neutral olefin (ca. 1.33 Å). This is exactly what we find if we look at the SOMO at the σ/π-TS (see Figure 5). Note that at the CASSCF level there is no need to localize spin and charge in σ/π-TS because the SOMO is already localized on one double

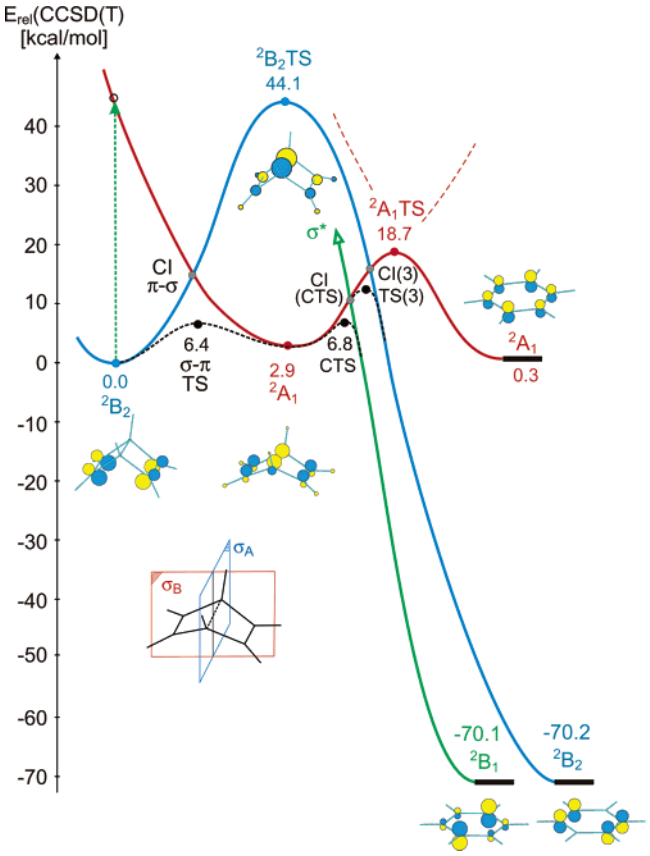

Figure 4. Potential surfaces involved in the conversion of $\mathbf{1}^{\bullet+}$ to $\mathbf{2}^{\bullet+}$. From left to right, the length of the bridging C−C bond in $\mathbf{1}^{\bullet+}$ increases. Energies of stationary points are from CCSC(T)/cc-pVTZ single-point calculations at CASSCF(5,6)/6-31G* optimized geometries (cf. Table 3). Orbital pictures represent the SOMOs in the respective states. Discussion, see text.

bond in the ground state of the π radical cation (see the discussion on symmetry breaking in the preceding section). As a consequence, the reaction is practically barrierless at the CASSCF level ($\Delta E^{\ddagger} = 1.1$ kcal/mol).

It is known that density functional methods have a problem with situations such as that which prevails in σ/π-TS. Due to incomplete cancellation of the odd electron's self-interaction,[38] DFT methods artifactually stabilize situations in radical ions where the spin is delocalized over situations where it is localized.[36,39,40] This feature may lead to abrupt changes in the electron distribution and hence to pronounced discontinuities in DFT potential surface, such as that illustrated in Figure 5 for the passage of $\mathbf{1}^{\bullet+}$ from the $^2B_2$ to the $^2A_1$ surface. Such discontinuities make it very difficult to locate the corresponding transition states. In fact, as shown in Figure 5, the σ/π-TS appears to lie *above* the conical intersection between the $^2B_2$ and the $^2A_1$ surfaces at the B3LYP level, which is of course nonsensical because, for purely topological reasons, this transition state should lie in the "moat" surrounding the conical intersection. Surprisingly, the B3LYP, CASSCF, and UMP2 geometries of the σ/π-TS do not differ significantly, and the B3LYP activation barrier is also not unreasonable, despite this strange behavior of the DFT method.

(38) Sodupe, M.; Bertran, J.; Rodriguez-Santiago, L.; Baerends, E. J. *J. Phys. Chem. A* **1999**, *103*, 166.
(39) Bally, T.; Sastry, G. N. *J. Phys. Chem. A* **1997**, *101*, 7923.
(40) Müller, B.; Bally, T.; Gerson, F.; de Meijere, A.; von Seebach, M. *J. Am. Chem. Soc.* **2003**, *125*, 13776.

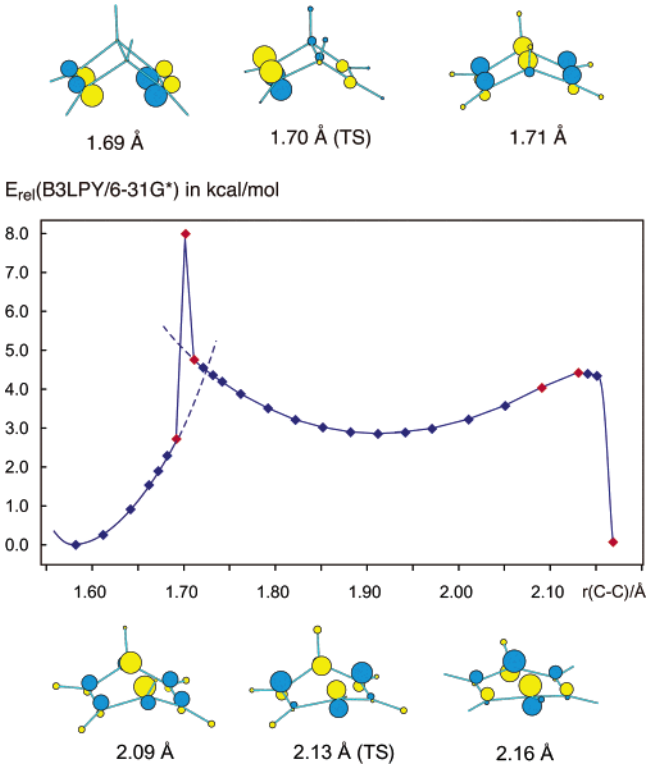

Figure 5. B3LYP potential curve for the rearrangement of $\mathbf{1}^{\bullet+}$ to $\mathbf{2}^{\bullet+}$. The pictures above and below show the SOMOs at the red points in the curve. Note the discontinuity of the surface at the first transition state, which is due to the necessity to localize spin and charge in one of the two double bonds of $\mathbf{1}^{\bullet+}$.

Second, the orbital correlation diagrams tell us that the $^2A_1$ state through which $\mathbf{1}^{\bullet+}$ transits on the way to $\mathbf{2}^{\bullet+}$ does *not* correlate with the ground state of $\mathbf{2}^{\bullet+}$, but with a $^2A_1$ *excited* state of the benzene radical cation (see the right side of Figure 1).[41] This state is actually reached if C_{2v} symmetry is retained while r_{C-C} is increased, via a transition state that lies 18.7 kcal/mol above the $^2A_1$ state of $\mathbf{1}^{\bullet+}$at the CCSD(T)/cc-pVTZ level. However, as the two JT components of the ground state of $\mathbf{1}^{\bullet+}$ have $^2B_2$ and $^2B_1$ symmetry (in C_{2v}), topology requires that, on the way to $\mathbf{2}^{\bullet+}$, the $^2A_1$ state must encounter *two* conical intersections with these two states and that there must consequently be *two* transition states leading from $\mathbf{1}^{\bullet+}(^2A_1)$ to the ground state of $\mathbf{2}^{\bullet+}$.

NHO, who look at the mechanism of the decay of $\mathbf{1}^{\bullet+}$ from the viewpoint of disrotatory vs conratatory pathways, have located one of these transition states (CTS in their nomenclature) which turns out to be that associated with the conical intersection CI(CTS) for crossing from the $^2A_1$ to the $^2B_1$ state at r_{C-C} = 2.25 Å. On the side of $\mathbf{1}^{\bullet+}$, the latter state corresponds to a (dissociative) $\sigma \rightarrow \sigma^*$ excited state (relative to the $^2A_1$ state of $\mathbf{1}^{\bullet+}$). Hence, to cross from the $^2A_1$ to the $^2B_1$ surface, the molecule must lose the symmetry plane σ_B (but may retain σ_A), and some coefficients in the SOMO must also go to zero, so that they can switch signs (cf. the SOMOs of the $^2A_1$ state of $\mathbf{1}^{\bullet+}$ and of the $^2B_1$ state of $\mathbf{2}^{\bullet+}$ in Figures 1 and 4). However, in contrast to the above-discussed case of σ/π-TS, no localization of spin and charge is required to pass from the $^2A_1$ to the $^2B_1$ surface; thus, DFT should be able to correctly describe this passage.

The CTS structure found by NHO has indeed nearly C_s symmetry (and can be reoptimized to a true transition state in C_s, see Supporting Information to this paper). The SOMO at this structure (Figure 5) shows that two of the coefficients that must switch sign are nearly zero, while the phase change at the bridgehead C−C bond has not yet taken place. As the potential surface becomes very steep just after crossing CTS and the wave function changes rapidly, we were not able to locate the point where the phase change takes place in the bridgehead bond.

As becomes evident from the above topological considerations and from Figure 4, there must, however, be another conical intersection of the $^2A_1$ state of $\mathbf{1}^{\bullet+}/\mathbf{2}^{\bullet+}$, this time with the $^2B_2$ state (labeled CI(3) in Figure 4) and an associated transition state, TS(3), that was not considered by NOH, although it is not a priori clear whether it is of relevance to the reaction under consideration. We have located CI(3) at the CASSCF level where it lies at r_{C-C} = 2.533 Å, just before $^2A_1$ TS (r_{C-C} = 2.558 Å), and about 10 kcal/mol above CI(CTS). As in the case of σ/π TS, finding the associated transition state is expected to be very difficult at the DFT level because the spin (and, formally, the associated charge) must once again localize in one of the two double bonds so that the SOMO can change its sign back to that required in a $^2B_2$ state. In addition, the b_2 MO that is an empty σ^* orbital on the side of $\mathbf{1}^{\bullet+}$ becomes doubly occupied in the $^2B_2$ of $\mathbf{2}^{\bullet+}$. All this makes that the electronic wave function changes very strongly and very rapidly in the vicinity of TS(3). Indeed, all our efforts to find that transition state proved futile, but from these calculations it became quite evident that TS(3) lies several kcal/mol higher than CTS. Thus, all we can say is that the decay of $\mathbf{1}^{\bullet+}$ to $\mathbf{2}^{\bullet+}$ possibly involves passage over both transition states, but as both pathways end on the same dynamical JT surface, it would in any event be very difficult to assess this branching experimentally.

Conclusion

We have observed the radical cation of Dewar benzene, $\mathbf{1}^{\bullet+}$, in a Freon glass at 77 K and in Ar matrices at 10 K. $\mathbf{1}^{\bullet+}$ distinguishes itself by a broad band at 600 nm which almost coincides with that of the related radical cation of norbornadiene, $\mathbf{3}^{\bullet+}$. This indicates a similarity of the electronic structure, i.e. the band corresponds in both cases to excitation of an electron from the bonding to the antibonding combination of olefinic π-MOs. Surprisingly, the CASSCF/CASPT2 method, which furnishes very good predictions of the electronic spectra of $\mathbf{1\text{-}Me_6}^{\bullet+}$ and $\mathbf{3}^{\bullet+}$ is in much poorer accord with experiment in the case of $\mathbf{1}^{\bullet+}$. We trace this to the fact that the CASSCF wave function for $\mathbf{1}^{\bullet+}$ (but *not* for $\mathbf{1\text{-}Me_6}^{\bullet+}$ and $\mathbf{3}^{\bullet+}$) breaks symmetry, and to the fact that the position of the visible band of $\mathbf{1}^{\bullet+}$is exceedingly sensitive to the dihedral angle between the two cyclobutene moieties.

That the radical cation of Dewar benzene, $\mathbf{1}^{\bullet+}$, persists in a Freon glass at 77 K for hours indicates that it is protected from the very exothermic decay to $\mathbf{2}^{\bullet+}$ by a barrier that must be >7 kcal/mol (assuming that $\Delta S^{\ddagger}$ for this rearrangement is close to zero). This is surprising because such exothermic radical ion rearrangements usually proceed spontaneously under these conditions.

(41) Actually, orbital correlation does not lead to the lowest excited $^2A_1$ state (where the totally symmetric π-MO of benzene depicted in Figure 4 is singly occupied), but to a higher-lying one. This is the reason for the barrier on the $^2A_1$ surface, which avoids a conical intersection between two $^2A_1$ states.

The reasons for this stability of $\mathbf{1}^{\bullet+}$ is that its ground state correlates actually with a *doubly excited* state of the same symmetry of $\mathbf{2}^{\bullet+}$ which makes for a high barrier for the ring-opening of $\mathbf{1}^{\bullet+}$ along a C_{2v} pathway. However, long before $\mathbf{1}^{\bullet+}$ reaches this barrier, the $^2A_1$ potential surface falls below that of the $^2B_1$ ground state, and the system crosses over to that surface, where the odd electron is now located in a bridging σ_{C-C}-MO, on its way to $\mathbf{2}^{\bullet+}$. That crossing involves a barrier of ca. 7 kcal/mol which is what protects $\mathbf{1}^{\bullet+}$ from spontaneous decay.

To get from the $^2A_1$ to the ground state of $\mathbf{2}^{\bullet+}$, the system must undergo yet another crossing to one of the two components of the JT active degenerate ground state of $\mathbf{2}^{\bullet+}$. According to calculations the crossing to the component which has B_1 symmetry occurs before and below that with the B_2 component and involves a lower-lying transition state. Thus, the simple ring-opening of $\mathbf{1}^{\bullet+}$ to $\mathbf{2}^{\bullet+}$ is one of the rare examples of a thermal reaction which involves two consecutive (avoided) state crossings. We would like to propose the term "pseudodiabatic" to distinguish such reactions from those which involve no pronounced changes in electronic structure on the way from reactants to products.

Methods

Synthesis. Dewar benzene **1** was synthesized according to the procedure of van Tamelen et al.[42] and purified by preparative GC (5% ODP on Chromosorb W) prior to use.

Low-Temperature Spectroscopy. A carefully degassed sample of pure **1** was warmed from 77 K until the vapor pressure had increased to 0.12 mbar (ca. −30°C), wherepon the sample was expanded into an evacuated 2-L glass bulb from where it was immediately condensed again into a tube held at 77 K. Subsequently, 5 mL of a degassed 1:1 mixture of $CFCl_3$ and CF_2BrCF_2Br[43] were condensed into the same tube to give a ca. 2×10^{-3} molar solution of **1** which was stored at −70 °C under Ar. Aliquots of this solution, which contained no trace of benzene according to GC/MS, were transferred under Ar into home-built low-temperature spectroscopy cells[44] where they were immediately frozen to 77 K. After taking reference spectra, the samples were exposed to a total dose of ca. 5 kSv of ^{60}Co radiation (1.173 and 1.332 MeV) in a Gammacell 220. Similar experiments were done with benzene to get reference spectra of the resulting radical cations.

In the matrix isolation experiments,[45] the results of which are shown in the Supporting Information, **1** was mixed with an equimolar amount of CH_2Cl_2 and a 1000-fold excess of a 9:1 mixture of Ar and N_2. The mixture was deposited on a CsI crystal held at ca. 20 K inside an APD Cryogenics closed-cycle cryostat. After depositing about 5 mMol of gas, the resulting matrix was cooled to ca. 8 K. IR spectra taken of these matrices showed no trace of benzene. To effect ionization of **1** the samples were exposed for 90 min to X irradiation (40 kV/40 mA, W anode).[44] The same experiment was done with benzene. Electronic absorption spectra were recorded on a Perkin-Elmer Lambda 900 instrument.

Photolyses were conducted either with a 250-W Hg medium-pressure lamp and appropriate cutoff filters, or with a 4-W Ar ion laser operated in multimode (485−515 nm).

Quantum Chemical Calculations. Geometries were optimized with the B3LYP density functional[46−48] and the CASSCF methods[49] as implemented in the Gaussian program package,[50] whereby the 6-31G* basis set was used, and selected symmetry elements were retained as indicated in the text. Some CASSCF optimizations and all excited-state CASPT2 calculations[51] were carried out with the MOLCAS suite of progams.[52] Thereby, an active space containing 5 electrons in 6 orbitals (2 π, 2 π*, 1 σ, and 1 σ*) was used (for some exploratory calculations, up to 13 electrons were correlated in 14 orbitals, but this hardly affected the results), and the ANO-S basis set was employed.[53] The CCSD(T)/cc-pVTZ single-point calculations were done with the Molpro program.[54] Molecular orbitals were rendered in a zero-overlap approximation using the MoPlot program.[55]

Acknowledgment. This paper is dedicated to Prof. Edwin Haselbach on occasion of his 65th birthday. We express our gratitude to the Swiss National Science Foundation for support of this research under Grant No. 200020-105217.

Supporting Information Available: (1) Text file: Cartesian coordinates and absolute energies, including thermal corrections, of all stationary points discussed in this study. (2) PDF file: Complete citations for refs 50 and 54; results of experiments in Ar matrices (Figure S1), potential curves for deforming $\mathbf{1}^{\bullet+}$ along the angle ω at different levels of theory (S2), dependence on the predicted excitation energies of $\mathbf{1}^{\bullet+}$ on ω (S3), and photoelectron spectrum of **1** and CASPT2 predictions (S4). This material is available free of charge via the Internet at http://pubs.acs.org

JA060176M

(42) van Tamelen, E. E.; Pappas, S. P.; Kirk, K. L. *J. Am. Chem. Soc.* **1971**, *93*, 6092.
(43) Sandorfy, C. *Can. J. Spectrosc.* **1965**, *10*, 85.
(44) Bally, T. Electronic Structure, Spectroscopy, and Photochemistry of Organic Radical Cations. In *Radical Ionic Systems*; Lund, A., Shiotani, M., Eds.; Kluwer: Dordrecht, 1991; p 3.
(45) Bally, T. Matrix Isolation. In *Reactive Intermediate Chemistry*; Moss, R. A., Platz, M. S., Jones, M., Eds.; John Wiley & Sons: Hoboken, NJ, 2004.
(46) Becke, A. D. *J. Chem. Phys.* **1993**, *98*, 5648.
(47) Lee, C.; Yang, W.; Parr, R. G. *Phys. Rev. B* **1988**, *37*, 785.
(48) Johnson, B. G.; Gill, P. M. W.; Pople, J. A. *J. Chem. Phys.* **1993**, *98*, 5612.
(49) Yamamoto, N.; Vreven, T.; Robb, M. A.; Frisch, M. J.; Schlegel, H. B. *Chem. Phys. Lett.* **1996**, *250*, 373.
(50) Frisch, M. J.; et al. *Gaussian 03*, Rev B.01; Gaussian, Inc.: Pittsburgh, 2003.
(51) Andersson, K.; Roos, B. O. CASPT2. In *Modern Electronic Structure Theory*; World Scientific Publ. Co.: Singapore, 1995; Vol. Part 1, Vol. 2; p 55.
(52) Karlström, G.; Lindh, R.; Malmqvist, P.-Å.; Roos, B. O.; Ryde, U.; Veryazov, V.; Widmark, P.-O.; Cossi, M.; Schimmelpfennig, B.; Neogrady, P.; Seijo, L. *Comput. Mater. Sci.* **2003**, *28*, 222.
(53) Pierloot, K.; Dumez, B.; Widmark, P.-O.; Roos, B. O. *Theor. Chim. Acta* **1995**, *90*, 87.
(54) Werner, H.-J.; Knowles, P. J.; et al. *Molpro*, version 2002.6 (see: http://www.molpro.net), Birmingham, UK., 2002.
(55) Olkhov, R. V.; Matzinger, S.; Bally, T. *MoPlot* (Molecular Orbital Plotting program), version 1.85 for Windows, Linux and MacOS X; University of Fribourg: Switzerland; see: http://www-chem-unifr.ch/tb/moplot/moplot.html, 2005.